Structured light scatteroscopy

Venkataramanan Krishnaswamy
Jonathan T. Elliott
David M. McClatchy, III
Richard J. Barth, Jr.
Wendy A. Wells
Brian W. Pogue
Keith D. Paulsen

Structured light scatteroscopy

Venkataramanan Krishnaswamy,[a],*
Jonathan T. Elliott,[a] David M. McClatchy III,[a]
Richard J. Barth Jr.,[b] Wendy A. Wells,[c]
Brian W. Pogue,[a] and Keith D. Paulsen[a]
[a]Dartmouth College, Thayer School of Engineering, 14 Engineering Drive, Hanover, New Hampshire 03755, United States
[b]Dartmouth College, Geisel School of Medicine, Department of Surgery, 1 Rope Ferry Road, Hanover, New Hampshire 03755, United States
[c]Dartmouth College, Geisel School of Medicine, Department of Pathology, 1 Rope Ferry Road, Hanover, New Hampshire 03755, United States

Abstract. A new imaging approach, structured light scatteroscopy (SLS), is demonstrated, which offers rapid wide-field imaging of microscopic morphological variations in bulk tissue surfaces. Elastic scattering of light offers exquisite sensitivity to ultrastructural changes at multiple size scales ranging from nanometers to millimeters, but in bulk tissues the confounding effects of molecular absorption and strong multiple scattering of light often lead to a dramatic reduction in scatter contrast and specificity. It is demonstrated that the SLS using structured high spatial frequency illumination and detection to probe the tissue achieves direct, absorption-independent, high-resolution maps of the scattering response. The scattering response is observed to be dependent on both the wavelength and spatial frequency of choice, indicating a potential for multiscale probing of ultrastructural changes in superficial tissue layers. This methodology can be easily applied in most wide-field imaging systems. © *The Authors. Published by SPIE under a Creative Commons Attribution 3.0 Unported License. Distribution or reproduction of this work in whole or in part requires full attribution of the original publication, including its DOI.* [DOI: 10.1117/1.JBO.19.7.070504]

The elastic scattering of light offers a highly sensitive probing mechanism to characterize changes in morphology and ultrastructure at various size scales ranging from nanometers to millimeters.[1,2] Creative ways to measure light scattering signals can allow macroscopic measurements to inform the microscopic and even submicroscopic properties of a variety of materials as diverse as metal surfaces and cell suspensions. However, in conventional wide-field imaging of dense random media, such as biological tissue, the sensitivity of scattered light to ultrastructural changes is often reduced by the strong influences of multiple scattering events and rendered less specific because of the confounding effects of molecular absorption by tissue chromophores such as hemoglobin, lipids, and water. While these absorbers can be diagnostically powerful, in many situations, such as in surgery, the ability to remove the effects of absorption (e.g., from the presence of surface blood) from the image and to simply visualize scatter changes would be valuable. Several confocal and specialized fiber-based scanning approaches[3,4] have been developed to probe or image optical property variations in cells and tissue surfaces. But almost all these techniques rely on semianalytical or empirical light-transport models to separate absorption effects from scattering. Direct measurement of light scattering signals using spatial and angular localization techniques has been proposed recently using a confocal and dark-field optical scheme.[5,6] However, a critical limitation of the approach is that the wide-field imaging (several centimeters) requires electro-optical or mechanical scanning, which is time consuming and cumbersome, and hence, impractical in many clinical applications.

To overcome these limitations, a wide-field localized imaging framework—termed structured light scatteroscopy (SLS)—is introduced, which is a modified version of the spatial frequency domain imaging (SFDI) approach[7,8] that is optimized for direct measurement of the localized light scattering response in bulk tissues. In contrast to the traditional SFDI approach, the SLS technique samples tissue responses only at high spatial frequencies (typically > 0.5 mm^{-1}). It is shown that such selective high spatial frequency probing makes the tissue response insensitive to variations in absorption and concomitantly very sensitive to scattering changes. Thus, this unique transport regime provides a direct means of extracting high-resolution scattering-sensitive signals without involving complex light transport models to separate the effects of absorption.

A schematic of the SLS technique is shown in Fig. 1(a). The core concept of SLS imaging is illustrated in Fig. 1(b), which shows simulated reflectance data from hypothetical tissue phantoms plotted as a function of sinusoidal spatial frequency values ranging from 0 to 1 mm^{-1}. The data were generated using the Virtual Photonics Simulator platform[9] using the standard Monte-Carlo based lookup table technique. Optical property values of $\mu_s' = 1$ and 4 mm^{-1} and $\mu_a = 0.016$ and 0.16 mm^{-1} were considered in all combinations, approximately matching the typical and extreme values found in breast tissue.[10]

Two distinct transport regimes can be seen in this plot: one where the measured reflectance for a given μ_s' value is sensitive to the change in background absorption and the other where it is largely insensitive to the change in background absorption. The SLS technique operates in the latter regime by controlling the minimum spatial frequency illumination that is used to probe, allowing direct measurements of the scattering response.

The minimum spatial frequency for SLS depends on the choice of the wavelengths used and the range of optical property variations observed in the target medium. For the range of optical properties typically observed in biological tissues at near-infrared wavelengths, as considered in the simulation here, the minimum spatial frequency required was approximately 0.5 mm^{-1}.

For experimental validation of SLS, a structured light imaging system[8] (Modulated Imaging Inc., Irvine, California) was used to project a set of high spatial frequency sinusoid patterns of light ranging from 0.5 to 1 mm^{-1} over a rectangular field of approximately 15×10 cm^2 and then recorded the resulting optical response. The system, though not optimized for rapid imaging, can achieve full-field SLS frame rates of ~5 to

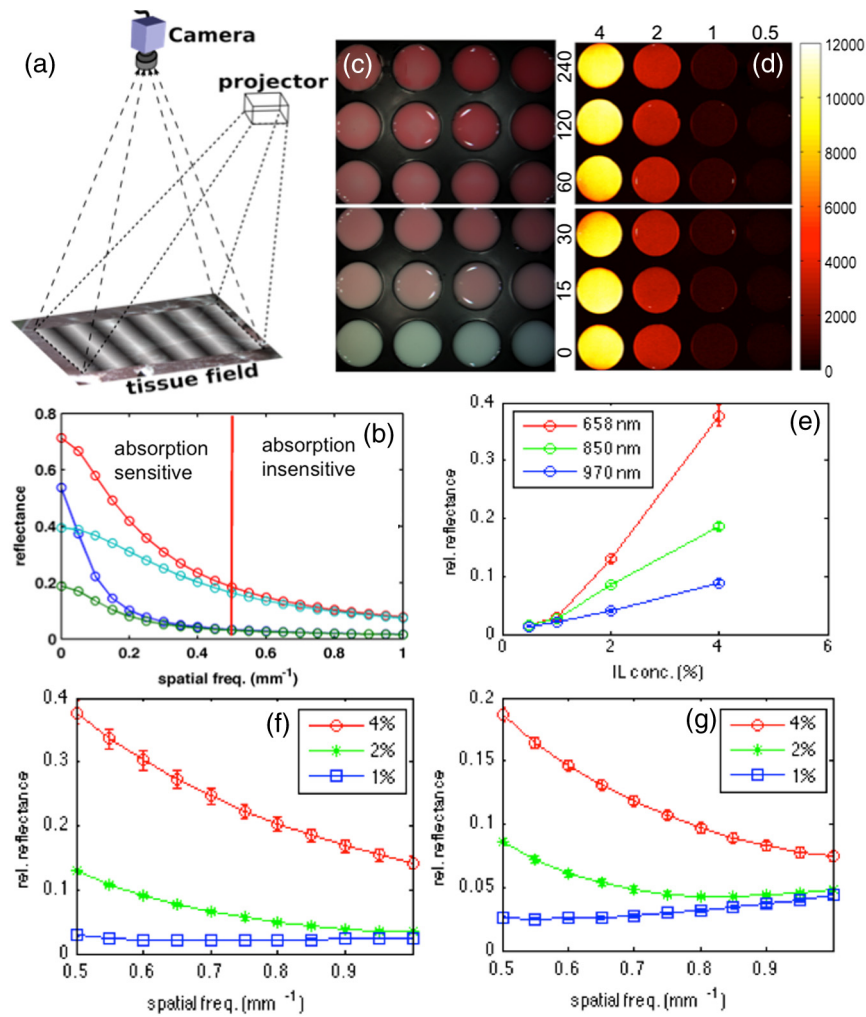*Address all correspondence to: Venkataramanan Krishnaswamy, E-mail: venkat.krishnaswamy@dartmouth.edu

Fig. 1 (a) A schematic of the structured light scatteroscopy (SLS) approach. (b) Plot of simulated reflectance versus spatial frequency. Colors green, dark blue, light blue, and red indicate $(\mu_a, \mu_s{}')$ values of $(0.016, 1)$, $(0.16, 1)$, $(0.016, 4)$, and $(0.16, 4)$ mm^{-1}, respectively. (c) Color photographic image of an intralipid and blood phantom matrices. The intralipid concentration varies along each row from 4 to 0.5%, whereas the blood concentrations vary down each column from 240 to 0 μM. (d) The SLS reflectance image of the same phantom matrix at 0.5 mm^{-1} spatial frequency and 730 nm wavelength showing negligible sensitivity to hemoglobin changes across the column. (e) Plot of measured average relative reflectance at 0.5 mm^{-1} spatial frequency versus intralipid concentration. (f and g) Plot of measured relative reflectance relative to a spectralon standard versus spatial frequency for 658 and 850 nm wavelengths, respectively. Error bars in all plots represent standard deviation in reflectance caused by variations in background blood absorption.

10 Hz per wavelength when imaging typical tissue specimens. At each spatial frequency, three phase-offset images, I_1, I_2, and I_3, were acquired at phase values of 0, $2\pi/3$, and $4\pi/3$, respectively, and the demodulated response, I_m, was readily obtained via[11]

$$I_m = [(I_1 - I_2)^2 + (I_1 - I_3)^2 + (I_2 - I_3)^2]^{1/2}. \quad (1)$$

To account for the instrument spatial frequency response and long-term drifts in source strength and detector sensitivity, relative reflectance (R_{rel}) images obtained by

$$R_{rel} = I_{sample}/I_{ref} \quad (2)$$

are typically considered for quantitative analysis, where I_{sample} and I_{ref} are the demodulated responses of the target and a spatially uniform reflectance standard, respectively.

To evaluate the SLS signal's sensitivity to scattering changes and its apparent insensitivity to absorption, a set of intralipid and blood phantoms was imaged with varying scattering and absorption properties. Heparinized whole porcine blood (Lampire Biologicals, Ottsville, Pennsylvania) with a hematocrit value of 12.6 g/dL was used to prepare a matrix of intralipid-blood phantoms. Intralipid concentrations were fixed at 0.5, 1, 2, and 4% lipids fraction corresponding to $\mu_s{}'$ values[12] of 0.5, 1, 2, and 4 mm^{-1}, respectively, at 660 nm, and the hemoglobin concentration in each case was varied from 0 to 240 μM. This range of intralipid concentrations adequately covers the scattering properties of breast tissues, and the hemoglobin range was 10 times greater than the typical average range observed in breast tissues.[10] The phantom matrix was imaged at a set of high spatial frequencies from 0.5 to 1 mm^{-1} in 0.05 mm^{-1} steps.

Figure 1(c) shows a color photo of the phantoms with hemoglobin concentration varying across the samples with fixed

intralipid concentration. Figure 1(d) presents the demodulated reflectance image acquired at a spatial frequency of $0.5~\text{mm}^{-1}$ and 658-nm wavelength, in which case the recovered SLS images reflect only the scattering variations and are insensitive to absorption changes in the phantoms. Figure 1(e) shows the average reflectance at $0.5~\text{mm}^{-1}$ spatial frequency plotted as a function of intralipid concentration and indicates a linear relationship between the recovered reflectance and the scatter concentration, similar to observed trends from probe-based localized scattering response measurements.[5] This linearity is lost at lower intralipid concentrations, where the signal change due to scattering was too small to be reliably measured using the off-the-shelf, uncooled CCD camera used in this study. Increasing the modulation depth of the input spatial frequency patterns or using a low noise, cooled CCD camera could help mitigate this issue.

Figures 1(f) and 1(g) show the spatial frequency and wavelength dependence of the scattered light referenced to a Spectralon reflectance standard. In localized scattering spectroscopy, the wavelength dependence of the recovered scatter parameters varies with the probe size and numerical aperture.[5] This dependency often results in varying scatter responses within the same medium when light is collected from different interrogation volumes because of differences in how the scattering phase function is sampled and provides a means to sense ultrastructural variations in heterogeneous media, such as tissue, at multiple size scales. In SLS, the effective sampling volume decreases as the spatial frequency is increased, so varying the spatial frequencies could provide a similar means to probe ultrastructural variations at multiple size scales. However, more studies examining the wavelength and spatial frequency dependence of the scattering response are required to improve our overall understanding of specific tissue ultrastructure influence, such as changes in nuclear and subcellular features versus in the extracellular matrix.

The advantage of SLS imaging was also demonstrated by interrogating a bovine tissue specimen (T-bone steak) before and after coating its surface with whole blood. The scattering contrast in this specimen is from the ultrastructural differences in bone, the surrounding spinal muscle tissue, fat, and connective tissues. Figures 2(a) and 2(b) show the color photographs of the imaged specimen before and after half of its surface was coated with whole blood, showing that the contrast in the scattering features beneath the layer of whole blood is suppressed due to the light absorption by the blood layer.

Figures 2(c) and 2(d) contain the SLS reflectance images obtained at $0.5~\text{mm}^{-1}$ spatial frequency, at the same wavelength where the contrast in scattering features is evident even in the regions visually masked by the layer of whole blood. The amount of blood on the tissue surface reflected an extreme case (even in surgical specimens); nonetheless, the SLS images still recovered the scatter features. A cut through of a human breast tissue specimen was also imaged using the SLS approach, following an Institutional Review Board approved protocol. Figure 2(e) shows a photograph of the specimen, and Fig. 2(f) shows the SLS image at $0.5~\text{mm}^{-1}$ spatial frequency, where the scattering contrast due to adipose and fibroglandular sections can be directly visualized.

Microscopic assessment of tissue morphological changes is the cornerstone of pathological analysis, providing contrast mechanisms for disease diagnosis and staging. Routine pathological evaluation involves extensive sample preparation and
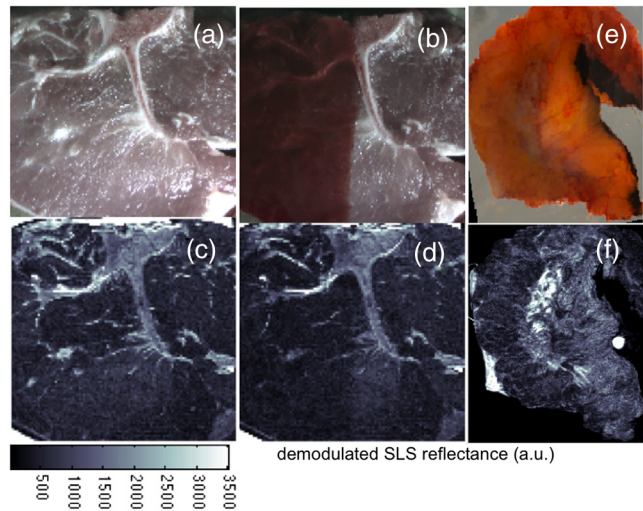

Fig. 2 (a) Photograph of a bovine tissue specimen. (b) The same specimen imaged after coating half of the imaging field with a thick layer of whole blood. (c and d) Corresponding $0.5~\text{mm}^{-1}$ spatial frequency SLS images at 658 nm. (e and f) Photograph and $0.5~\text{mm}^{-1}$ SLS image at 658 nm acquired from a cut-through section of a breast mastectomy surgical specimen.

processing, which makes it impractical for clinical applications where near real-time evaluation is needed. Imaging systems that can provide real-time assessment of pathologies could inform clinical procedures. The SLS imaging enables rapid, noninvasive, wide-field morphological assessment in tissue surfaces, which when validated against pathology could offer potential clinical use.

References

1. W. Qian et al., "Dark-field light scattering imaging of living cancer cell component from birth through division using bioconjugated gold nanoprobes," *J. Biomed. Opt.* **15**(4), 046025 (2010).
2. L. J. Johnson, D. F. Hanley, and N. V. Thakor, "Optical light scatter imaging of cellular and sub-cellular morphology changes in stressed rat hippocampal slices," *J. Neurosci. Methods* **98**(1), 21–31 (2000).
3. I. Itzkan et al., "Confocal light absorption and scattering spectroscopic microscopy monitors organelles in live cells with no exogenous labels," *Proc. Natl. Acad. Sci. U. S. A.* **104**(44), 17255–17260 (2007).
4. M. R. Austwick et al., "Scanning elastic scattering spectroscopy detects metastatic breast cancer in sentinel lymph nodes," *J. Biomed. Opt.* **15**(4), 047001 (2010).
5. V. Krishnaswamy et al., "Scanning in situ spectroscopy platform for imaging surgical breast tissue specimens," *Opt. Express* **21**(2), 2185–2194 (2013).
6. A. M. Laughney et al., "Scatter spectroscopic imaging distinguishes between breast pathologies in tissues relevant to surgical margin assessment," *Clin. Cancer Res.* **18**(22), 6315–6325 (2012).
7. D. J. Cuccia et al., "Modulated imaging: quantitative analysis and tomography of turbid media in the spatial-frequency domain," *Opt. Lett.* **30**(11), 1354–1356 (2005).
8. D. J. Cuccia et al., "Quantitation and mapping of tissue optical properties using modulated imaging," *J. Biomed. Opt.* **14**(2), 024012 (2009).
9. "Virtual Tissue Simulator software package," www.virtualphotonics.org/vts/ (November 2013).
10. S. L. Jacques, "Optical properties of biological tissues: a review," *Phys. Med. Biol.* **58**(11), R37 (2013).
11. M. A. A. Neil, R. Juskaitis, and T. Wilson, "Method of obtaining optical sectioning by using structured light in a conventional microscope," *Opt. Lett.* **22**(24), 1905–1907 (1997).
12. R. Michels, F. Foschum, and A. Kienle, "Optical properties of fat emulsions," *Opt. Express* **16**(8), 5907–5925 (2008).